Copy 1

NATIONAL ADVISORY COMMITTEE FOR AERONAUTICS

WARTIME REPORT

ORIGINALLY ISSUED
January 1943 as
Advance Confidential Report

THE EFFECT ON STABILITY AND CONTROL OF A PUSHER PROPELLER BEHIND CONVENTIONAL TAIL SURFACES AS DETERMINED BY TESTS OF ~~A POWERED~~ MODEL IN THE FREE-FLIGHT TUNNEL

By John P. Campbell and Thomas A. Hollingworth

Langley Memorial Aeronautical Laboratory
Langley Field, Va.

WASHINGTON

NATIONAL ADVISORY COMMITTEE FOR AERONAUTICS

ADVANCE CONFIDENTIAL REPORT

THE EFFECT ON STABILITY AND CONTROL OF A PUSHER PROPELLER BEHIND CONVENTIONAL TAIL SURFACES AS DETERMINED BY TESTS OF A POWERED MODEL IN THE FREE-FLIGHT TUNNEL

By John P. Campbell and Thomas A. Hollingworth

SUMMARY

The effects on stability and control of a pusher propeller behind conventional horizontal and vertical tail surfaces have been determined in the NACA free-flight tunnel by tests of a 1/10-scale model of an NACA submerged-engine pusher airplane design. The investigation consisted of flight and balance tests at windmilling and high-power conditions with a partial-span Zap extensible flap extended and retracted. The effects of changes in vertical-tail area, horizontal-tail incidence, and center-of-gravity location were also determined.

The tests showed that, with a pusher propeller located behind the tail surfaces, power caused only minor changes in stability and control. The windmilling propeller provided slight increases in longitudinal and directional stability. Application of power only slightly affected the longitudinal stability, increased the directional stability, and necessitated a small amount of aileron trim. The dihedral effect, stalling behavior, and rudder trim were not affected by power.

This particular pusher design with the propeller behind the tail surfaces is considered very promising as a means of eliminating the undesirable slipstream effects of tractor propellers.

INTRODUCTION

The trend toward more powerful engines in single-engine military airplanes has caused the propeller-slipstream effects on stability and control to become increasingly important.

Because these slipstream effects are, on the whole considered undesirable, means are being sought to eliminate them. One apparent solution to the problem is the use of pusher propellers. Various designs to permit the use of pusher propellers have been proposed, such as the tailless and tailfirst airplanes. The NACA has recently suggested a submerged-engine pusher design with the propeller directly behind conventional horizontal and vertical tail surfaces. A 1/10-scale powered model of this design has been tested in the NACA free-flight tunnel to determine the effect of such a propeller arrangement on stability and control characteristics. During the investigation, a special effort was also made to observe any changes in stability and control that might have been caused by the short tail length inherent in the design.

APPARATUS AND METHODS

Wind Tunnel

The investigation was carried out in the NACA free-flight tunnel described in reference 1. Photographs of the test section of the tunnel show models being tested in flight in figure 1 and on the balance in figure 2.

In the flight tests, the model flies freely in the tunnel under the remote control of a pilot seated at the bottom and rear of the tunnel. An operator at the side of the tunnel adjusts the airspeed, tunnel angle, and power to the motor in the model to correspond to the desired flight conditions. After the lateral and longitudinal trim of the model has been adjusted for the particular conditions, the stability of the model in uncontrolled flight is observed and the effectiveness of the controls is determined. In order to supplement the pilot's observations, moving-picture records of flights are taken by three cameras mounted at the top, side, and rear of the tunnel.

The balance tests were run on the free-flight tunnel six-component balance. The balance rotates with the model in yaw so that all forces and moments are measured with respect to the stability axes.

Model

The 1/10-scale model of the NACA submerged-engine pusher airplane design used in the tests was constructed and prepared for the testing by the NACA. A three-view drawing of the model is presented as figure 3 and photographs of the model are shown in figures 4 and 5. The dimensional characteristics of the airplane as scaled up from the model values are given in table I.

In addition to the vertical tails specified for the airplane (tails 1 and 2 of fig. 3), a larger vertical tail (tail 3) was installed on the model for some of the tests. Only the upper vertical tail was provided with a movable rudder.

A simple wire landing gear was installed on the model as shown in figure 3 to provide sufficient ground angle for take-off and to absorb shock in landings.

The weight of the model after final preparation and balancing was about 5.80 pounds, which corresponded to 5800 pounds for the airplane. The center of gravity of the model was adjusted to 24.2 percent of the mean aerodynamic chord. The moments of inertia of the model corresponded to those of typical modern fighter airplanes as indicated by the ratios of wing span to radii of gyration shown in table I.

Electromagnets were installed in the model to provide abrupt deflections of the ailerons, rudder, and elevator. The ailerons were deflected with an equal up-and-down movement varying from $\pm 12^\circ$ to $\pm 18^\circ$. Rudder deflections varying from $\pm 10^\circ$ to $\pm 20^\circ$ were used in conjunction with the ailerons to provide proper control coordination. For longitudinal control abrupt elevator deflections of $\pm 2^\circ$ or $\pm 3^\circ$ were used.

The model was powered by a direct-current, controllable-speed electric motor rated 1/5 horsepower at 15,000 rpm and geared with a ratio of 2.54:1 to a pusher propeller. The motor was placed forward of the wing and was connected to the propeller by a 5/16-inch-diameter, hollow, aluminum drive shaft about 18 inches long.

An adjustable-pitch, two-blade, 11-inch wood propeller was used on the model. For all the power tests, the blade angle at 0.75 radius was set at 24° in order to absorb full power at maximum efficiency with the desired propeller speed of 6000 rpm.

Test Conditions

The power characteristics of the model motor and gear box unit were determined by Prony brake tests and the characteristics of the propeller with various amounts of pitch were ascertained at dynamic pressures of 0, 1.90, and 4.09 pounds per square foot. These tests indicated that a blade angle of 24° at 0.75 radius would most nearly satisfy the required conditions. For each of the flight and balance tests the power supplied to the model was adjusted to the desired condition by varying the input voltage.

The flight tests covered a range of airspeeds from 25 to 50 miles per hour, which corresponded to 80 to 160 miles per hour for the airplane represented. The power was varied from windmilling to 0.235 brake horsepower, which was the maximum obtainable from the motor used in the model. The thrust developed in the flight tests was determined from the difference between the flight-path angle, or tunnel angle, with power on and the angle with propeller off at the same lift coefficient. The high-power condition in the flight tests corresponded to about 550 brake horsepower for the airplane.

Most of the balance tests were run at a dynamic pressure of 4.09 pounds per square foot, which corresponds to a velocity of about 40 miles per hour under standard sea-level conditions and to a test Reynolds number of about 209,000 based on the mean chord of 0.583 foot. The high-power tests were run at a dynamic pressure of 1.90 pounds per square foot in order to represent greater airplane horsepower and thereby extend the power range of the tests. For each balance test, the power to the model was adjusted to correspond to 1100 brake horsepower for the airplane. This power adjustment was made by varying the voltage to give the proper values of thrust coefficient T_c at each lift coefficient. The desired thrust horsepower (and then the thrust coefficient) for each lift coefficient was computed by multiplying the rated airplane horsepower (1100 bhp) by a propeller efficiency corresponding to the particular lift coefficient. Propeller efficiencies of an airplane with a speed range similar to that of this airplane were used in making these computations. The variations of thrust coefficient, torque coefficient, and propeller efficiency with lift coefficient are shown in figure 6.

SYMBOLS

C_L lift coefficient (L/qS)

C_D drag coefficient (D/qS)

C_Y lateral-force coefficient (Y/qS)

C_n yawing-moment coefficient $\left(\frac{\text{yawing moment}}{qbS}\right)$

C_l rolling-moment coefficient $\left(\frac{\text{rolling moment}}{qbS}\right)$

C_m pitching-moment coefficient $\left(\frac{\text{pitching moment}}{qcS}\right)$

L lift, pounds

D drag, pounds

Y lateral force, pounds

q dynamic pressure, pounds per square foot $(\frac{1}{2}\rho V^2)$

c average chord, feet

S wing area, square feet

b wing span, feet

C_{l_β} rate of change of rolling-moment coefficient with sideslip, per radian

C_{n_β} rate of change of yawing-moment coefficient with side-slip, per radian

β angle of sideslip, radians

ψ angle of yaw, degrees

α angle of attack of fuselage reference line, degrees

T_c thrust coefficient $\left(\frac{T}{\rho V^2 D^2}\right)$

T	thrust, pounds
ρ	air density, slugs per cubic foot
V	airspeed, feet per second
D	propeller diameter, feet
Q_c	torque coefficient $\left(\frac{Q}{\rho V^2 D^3}\right)$
Q	torque, pound-feet
δ_{a_r}	right aileron deflection, degrees
δ_e	elevator deflection with respect to stabilizer chord, degrees
p	rolling velocity, radians per second
$\frac{pb}{2V}$	helix angle generated by wing tip in roll, radians
i_t	angle of stabilizer setting, degrees
η	propeller efficiency
C_{l_p}	rate of change of rolling-moment coefficient with the helix angle $\frac{pb}{2V}$

TESTS AND RESULTS

The stability and control characteristics of the model were investigated at the windmilling and high-power conditions and with the propeller removed. Tests were made with the partial-span Zap flap retracted and fully extended and with various combinations of the vertical tails shown in figure 3.

A few preliminary tests were made to improve the longitudinal stability of the model with flaps down. During these tests the center of gravity was moved forward from 24.2 to 19.7 percent of the mean aerodynamic chord and the horizontal-tail incidence was changed from -5° to 0°. Tuft tests were made to determine the stalling characteristics of the wing and horizontal tail.

Flight tests.- The longitudinal data obtained in the flight tests are presented in figure 7 in the form of elevator deflections required for trim at different lift coefficients. The curves of figure 7 show the effect of flap deflection and power on longitudinal trim. The effectiveness of the ailerons for lateral control was determined by noting the deflections required for good control in the tunnel flights and by measuring from moving-picture records the rolling velocities produced both in abrupt aileron maneuvers with rudder fixed and in the recoveries from these maneuvers. The values of $pb/2V$ obtained in these tests are presented in table II.

Balance tests.- The results of the balance tests are given in figures 8 to 11. The curves of figure 8 show the effects of power and flaps on the aerodynamic characteristics of the model. The longitudinal data from this figure are replotted in figure 9 to show more clearly the effects of power and flap deflection on longitudinal stability and trim. The changes in longitudinal stability caused by variation of horizontal-tail incidence and center-of-gravity location are shown in figure 10. The results of balance tests made to determine the elevator effectiveness are shown in figure 11. The lateral-stability characteristics of the model as affected by power, flaps, and fin area are given in figures 12 and 13 in the form of rolling-moment, yawing-moment, and lateral-force coefficients plotted against angle of yaw at a lift coefficient of 0.75. The slopes of the rolling-moment and yawing-moment curves of figures 12 and 13 are shown in figure 14 on a plot of C_{l_β} against C_{n_β} together with approximate boundaries for neutral spiral stability ($E = 0$) and for neutral oscillatory stability ($R = 0$). The effectiveness of the lateral control as determined by balance tests is shown in figure 15 in the form of rolling-moment and yawing-moment coefficients plotted against right aileron deflection.

Tuft tests.- The results of tuft tests made to determine the stalling characteristics of the wing and horizontal tail are presented in figure 16.

DISCUSSION

Preliminary Tests

Because of the short tail length of the model, the horizontal tail was originally set at an angle of incidence of -5° to avoid excessive up-elevator travel for trim with flaps down. With this tail incidence, deflection of the partial-span Zap flap caused the model to become statically longitudinally unstable. Sustained flights were impossible at any airspeed because of divergences in pitch that could not be controlled by elevator deflection. Moving the center of gravity forward from 24.2 to 19.7 percent of the mean aerodynamic chord made the model longitudinally stable at lift coefficients above 0.80 and good flights could be made without using elevator control. At lower lift coefficients, however, sustained flights could be made only by continually applying alternate up-and-down elevator deflections to prevent the model from diverging. At lift coefficients below 0.50, moreover, the stability was not sufficient to permit flights to be made even in this manner.

The character of this instability suggested a form of tail stalling. When the horizontal tail was set at -5°, the downwash at low angles of attack was believed to be sufficient to cause the lower surface of the tail to stall. This belief was substantiated by the behavior of the model on the floor before take-off. The model often assumed a negative angle of attack before taking off and from this attitude the nose could not be brought up by elevator control. In these cases the lower surface of the tail was evidently fully stalled instead of intermittently stalled as it appeared to be in flight.

The tuft tests made to determine the stalling characteristics of the wing and of the upper and lower surfaces of the horizontal tail proved that the assumptions regarding tail stalling were correct. The results of these tests, presented in figure 16, indicate that the lower surface of the tail was almost completely stalled at an angle of attack of -4° and that the outer portion was stalled at 0°. This tail stalling accounts for the difficulty encountered in flights at lift coefficients below 0.80. The unstalled condition at angles of attack of 4° and 6° explains the improved longitudinal behavior of the model at higher lift coefficients. It is realized that the tail stalling of the

airplane would occur at much higher negative angles of attack of the tail and that the model test results cannot be used quantitatively but may be taken only as an indication of an unsatisfactory condition that would be encountered by the airplane if too great a negative tail incidence were used.

Changing the horizontal-tail incidence to 0° eliminated the tail stalling (fig. 16) and made the model longitudinally stable with flaps down at all lift coefficients with the 24.2 percent center-of-gravity location. The flight-test longitudinal-trim curves of figure 7 indicate that the stability was slightly less for the flaps-down condition than for the flaps-up condition. No difficulty was experienced in making flights with flaps down, however, and the stability was considered entirely adequate.

The results of balance tests (figs. 8 and 10) show the changes in stability with flap deflection. In figure 10, the unstable pitching-moment slope for the flaps-down condition with the original tail incidence and center-of-gravity position explains the inability to obtain flights at this condition. The manner in which the forward shift in center-of-gravity position increased the stability is also shown in this figure. As indicated by the flight tests at this condition, the stability is positive at the high lift coefficients but only about neutral at lift coefficients below 0.80. The pronounced stabilizing effect caused by the change to 0° tail incidence is as evident in the results of balance tests (fig. 10) as in the flight tests.

Longitudinal Stability

Increasing the power caused only a slight change in the static longitudinal stability for both the flaps-up and flaps-down conditions, as shown by the curves of figures 7, 8, and 9. It appears from the longitudinal trim data obtained in the flight tests (fig. 7) that the static stability as indicated by the elevator deflections required to trim at different lift coefficients was slightly increased by power with flaps up and very slightly decreased by power with flaps down. The balance test results presented in figures 8 and 9 agree fairly well with the flight results in this respect and show even smaller changes in stability with power. The windmilling propeller appears to have provided a slight increase in longitudinal stability for all conditions.

Application of power caused opposite changes in longitudinal trim for the flaps-up and flaps-down conditions. The trim changes were apparent in the flight tests when successive flights were made at the windmilling and high-power conditions with a constant elevator setting. Application of power caused the trim airspeed to increase with flaps up and to decrease with flaps down. These trim changes are shown by the curves of figures 7 and 9.

The damping of the phugoid oscillation was satisfactory for all power conditions and appeared to be slightly better at high power.

Longitudinal Control

The longitudinal control appeared to be good in all respects despite the short tail length of the model and the nearness of the propeller to the horizontal tail. Abrupt elevator deflections of only ±2° or ±3° were required to correct for longitudinal disturbances and to maneuver the model in the tunnel as desired. Slightly greater elevator deflections have been required on most other models tested in the free-flight tunnel.

The elevator-trim characteristics as indicated by the flight data in figure 7 appear to be very good. Trim for the high-speed condition to the stall was obtained without excessive elevator travel but a fairly large increase in elevator movement was required to produce the stall. These elevator characteristics are considered desirable.

The balance-test results in figure 11 show that, with power on, the values of $\frac{dC_m}{d\delta_e}$ were about -0.013 with flaps up and -0.015 with flaps down. These values divided by $\frac{dC_m}{dC_L}$ for the corresponding conditions give values of $\frac{dC_L}{d\delta_e}$ of 0.084 with flaps up and 0.177 with flaps down. These values of $\frac{dC_L}{d\delta_e}$, which are in fairly good agreement with the flight-test results, indicate adequate elevator effectiveness for the particular degrees of static stability $\left(\frac{dC_m}{dC_L}\right)$ afforded by the 24.2 percent center-of-gravity location.

Stalling Characteristics

The behavior of the model at the stall was not noticeably affected by power and was considered satisfactory at all conditions of flaps and power.

With the flaps up, the behavior at the stall was not consistent. At times a definite warning of the stall was observed in the form of a slight pitching motion, but at other times the model would roll off to either side at the stall without warning. The stall was, however, gentle in all cases and caused no great difficulty.

When the flaps were down, the stalling characteristics were excellent. Ample warning of the stall was afforded by a noticeable pitching motion, and the stall itself was evidenced by a slow dropping of the model to the floor of the tunnel. Even with the stall sufficiently advanced to cause this gradual loss of altitude, the ailerons were still effective in picking up a low wing. The results of the tuft tests shown in figure 16 provide a plausible explanation for the good stalling behavior with flaps down. The stall diagrams indicate that the upper surface of the large partial-span Zap flap and the portion of the wing ahead of it stall well before the ailerons. The apparent stalling of the horizontal tail at high angles of attack as indicated by the tuft tests was actually a form of tail buffeting and was probably responsible for the pitching motions that warned of the stall.

Lateral Stability

Effect of Power.- Power provided a noticeable increase in directional stability and a slight increase in dihedral effect. In the flight tests, these stability changes were evidenced by the smoother, steadier flights obtained with power on. When, during a single continuous flight, the power was increased gradually from windmilling to high power, a definite steadying of the model, especially in yaw, could be observed. This effect of power, which was noted in flights with flaps either up or down, was considered beneficial in improving the flight behavior of the model.

The spiral stability, which was satisfactory with power off, did not appear to be affected by power. With the flaps up and only the upper vertical tail on, power definitely improved the oscillatory stability and reduced the adverse yawing caused by the ailerons.

The balance-test results in figures 12, 13, and 14 substantiate the observations made in the flight tests in regard to the effect of power on the lateral-stability characteristics of the model. The yawing-moment curves of figure 12 have greater slopes with power on and, in addition, the curves are straightened out by power at the higher angles of yaw. This straightening out with power on suggests that the propeller was acting in such a manner as to delay the stalling of the vertical tails. At the low angles of yaw, however, the effect of power in increasing the directional stability cannot be credited to the change in air flow over the tail surfaces because, as shown in figure 13, most of the increase was obtained with the tails removed. Neither can the major portion of the increase in directional stability with power on be attributed to the propeller normal force. The balance tests with tails removed indicated a much larger increase in lateral force in changing from the propeller-off to the windmilling condition than in changing from the windmilling to the high-power condition. In this respect the tests agree well with propeller theory. On the other hand, the increase in directional stability (C_{n_β}) provided by the windmilling propeller was less than one-half as great as the C_{n_β} increase produced by the application of power. These results indicate that the inflow to the powered pusher propeller might have affected the air flow over the fuselage in such a way as to reduce its unstable yawing moment without appreciably changing its side force. It is interesting to note in figures 13 and 14 that, with all tails removed, power provided enough fin effect to balance the unstable moment of the wing-and-fuselage combination and thereby make the model neutrally directionally stable.

The curves of figures 12 and 13 show the slight increase in dihedral effect provided by power. The increase appears to be substantially the same for flaps up or down and is almost negligible in either case.

The summary of the balance results given in figure 14 indicates the reasons for the flight-test observations regarding the effects of power on spiral and oscillatory stability. Inasmuch as power increases both C_{n_β} and $-C_{l_\beta}$, it causes a shift on the stability plot (G to H or E to F) approximately parallel to the spiral-stability boundary and thereby affects the spiral stability very little. The improvement in oscillatory stability caused by power with flaps

up and only the upper vertical tail on is shown graphically in figure 14 by the shift from condition D, near the oscillatory-stability boundary, to condition I, well away from that boundary and apparently in a very stable region.

In general, the effects of power on the lateral stability of this model were considerably less than the effects of power on the stability of conventional tractor models tested in the free-flight tunnel. The changes, moreover, were in no case detrimental and were in some cases definitely beneficial to the flight behavior of the model. In this respect, this particular pusher design appears to be completely justified.

Effect of flaps.- The results of balance tests given in figure 12 show that flap deflection caused a considerable reduction in dihedral effect as expected but did not affect the directional stability. It appears from figure 14 that this reduction in dihedral effect should have caused the model to become spirally unstable.

An analysis of the $pb/2V$ values in table II also reveals evidence of slight spiral instability with flaps down. For the flaps-down condition, the values of $pb/2V$ obtained during recoveries from abrupt aileron maneuvers were somewhat lower than the values obtained during the maneuvers themselves. This reduced aileron effectiveness may be taken as an indication of spiral instability, because the aileron rolling velocity was evidently reinforced by an unstable rolling in abrupt maneuvers starting from a wing-level attitude and opposed by the same rolling during recoveries. Inasmuch as the variation of the $pb/2V$ values with flaps up was the reverse of that with flaps down, the model is, by the same reasoning, judged to be spirally stable for the flaps-up condition.

The spiral instability with flaps down was apparently very slight, as no definite indications of it could be noted in the uncontrolled-flight tests. At any rate, the condition was certainly not objectionable and the flight behavior of the model with flaps down was considered entirely satisfactory.

In regard to the question of spiral stability, it should be pointed out that tests of several models in the free-flight tunnel have shown that slight spiral instability is not objectionable. The rates of spiral divergence with moderate fin area and only slightly positive dihedral effect are usually

so small as to cause no difficulty in free-flight tunnel tests. The pronounced spiral instability usually caused by negative dihedral effect is, however, considered definitely undesirable.

Effect of vertical-tail area.- In spite of the short tail length of the model, adequate directional stability was obtained with relatively small vertical tails (tails 1 and 2 of fig. 3). For all conditions of power and flaps, no objectionable adverse yawing was noted when ailerons alone were used for lateral control. The damping of the lateral oscillations was also satisfactory.

When the tail area was increased 60 percent by replacing the upper tail with a larger tail of the same aspect ratio (tail 3 of figs. 3 and 4), only a slight improvement in the flying characteristics was noted. This improvement was not considered sufficient to justify the increase in area.

When the tail area was decreased 50 percent by removing the lower tail, the model retained a small amount of directional stability. In windmilling-power flights with the flaps up and with the ailerons used alone for control, the small upper tail alone did not, however, provide enough fin effect to keep the adverse yawing from becoming excessive. When the propeller was removed sustained flights with the single tail were almost impossible because of the pronounced effects of adverse yawing. During a continued application of aileron control in flights with propeller off and rudder fixed, the model would at times yaw adversely to a large angle, roll against the ailerons, and drop to the floor. The stability at both the propeller-windmilling and propeller-off conditions was considered unsatisfactory with the single tail with flaps up. With the flaps down or with power on, the flight behavior of the model with the single tail was much improved and the adverse yawing was never great enough to cause loss of aileron control.

The balance test results in figures 13 and 14 show the increase in directional stability provided by the small vertical tails. Together the tails increased C_{n_β} by about 0.075, which resulted in a C_{n_β} value of about 0.055 for the complete airplane with power off.

Lateral Control

The lateral control of the model was not noticeably affected by power, except that a slight amount of aileron

trim was required to balance propeller torque. For the high-power condition in the flight tests, a total aileron deflection of 5° right was required for lateral trim. Power apparently did not affect the directional trim, inasmuch as no change in rudder setting was necessary in going from windmilling power to high power. The rudder control was not noticeably affected by power despite the proximity of the propeller to the vertical tails.

On the basis of the abrupt aileron deflections required for satisfactory control in the flight tests, the lateral control of the model was considered entirely adequate. In fact, considerably smaller aileron deflections were needed during the tests than are required for the average model flown in the free-flight tunnel. It should be pointed out, however, that the area of these plain ailerons is 8.8 percent of the wing area, which is somewhat greater than the average aileron area of present-day airplanes. A reduction in this area could probably be made without rendering the aileron control inadequate.

The values of $pb/2V$ shown in table II are further proof of the adequacy of the aileron control of the model. With the assumed total aileron movement of 45° and the rudder fixed, the $pb/2V$ values are well above the minimum required value of 0.070. Flap deflection caused a substantial improvement in the rolling velocities obtained with the ailerons. The slight reduction in aileron effectiveness during recoveries with flaps down, which has been attributed to slight spiral instability, was not considered serious inasmuch as the $pb/2V$ was still greater than for any flap-up condition. It can be seen from the balance results of figure 15 that a rolling-moment coefficient of about 0.026 was provided by the equal up-and-down aileron deflection of $\pm 12\frac{1}{2}^{\circ}$ that was used in the tests to determine the aileron rolling velocities. A C_{l_p} value of 0.54 for the model with flaps up is obtained by dividing this value of C_l (0.026) by the corresponding $pb/2V$ value (0.048).

Abrupt rudder deflections varying from ±10° to ±20° were required for good control coordination depending upon the particular flight condition. The larger rudder deflections were used with the larger aileron deflections at low airspeeds. These rudder deflections were only slightly larger than those required on the average conventional tractor models tested in the free-flight tunnel, even though only the upper tail of the model was equipped with a rudder.

The short tail length of this design does not appear to necessitate large rudder areas or rudder deflections. In fact, smaller rudder areas and deflections might well be possible inasmuch as no rudder trim is required for high-power flight.

With the ailerons fixed, the rudder provided a fair amount of lateral control with the flaps up. Recovery from angles of bank as high as 8° or 10° could be accomplished without excessive change in heading. With the flaps down, however, the rudder was virtually ineffective in rolling the model and could not pick up a low wing even at very small angles of bank.

CONCLUDING REMARKS

The effects of power on the stability and control characteristics of the pusher model with the propeller behind the tail surfaces may be summarized as follows:

1. Longitudinal stability and trim were only slightly affected by power.

2. Power caused a substantial increase in directional stability but did not appreciably change the effective dihedral.

3. The stalling characteristics were not affected by power.

4. In power-on flights a small amount of aileron trim was required, but no rudder trim was necessary.

5. The windmilling propeller provided slight increases in longitudinal and directional stability.

In spite of the short tail length that was necessary with this pusher-propeller arrangement, the general flight behavior of the model was considered excellent. A horizontal tail only slightly larger than normal provided satisfactory longitudinal stability; ample directional stability and control were afforded by vertical tails of normal size. These tests, therefore, indicated that the use of a short tail length did not materially increase the difficulty of obtaining good stability and control characteristics.

On the basis of the free-flight tunnel tests, it appears that the undesirable effects of power on stability and control can be eliminated by placing a pusher propeller behind conventional horizontal and vertical tail surfaces.

Langley Memorial Aeronautical Laboratory,
National Advisory Committee for Aeronautics,
Langley Field, Va.

REFERENCE

1. Shortal, Joseph A., and Osterhout, Clayton J.: Preliminary Stability and Control Tests in the NACA Free-Flight Wind Tunnel and Correlation with Full-Scale Flight Tests. T.N. No. 810, NACA, 1941.

TABLE I

DIMENSIONAL CHARACTERISTICS OF NACA SUBMERGED-ENGINE PUSHER AIRPLANE AS REPRESENTED BY 1/10-SCALE MODEL TESTED IN NACA FREE-FLIGHT TUNNEL

Engine:	
Horsepower, rated	1100
Propeller:	
Diameter, feet	9
Number of blades	2
Weight, pounds	5800
Wing:	
Area, square feet	226
Span, feet	39
Aspect ratio	6.73
Airfoil section -	
Root	NACA 67,1-116
Dihedral break	NACA 67,1-116
Tip	NACA 67,1-115
Incidence -	
Root, degrees	3
Dihedral break, degrees	3
Tip, degrees	1
Dihedral of outer panel, degrees	6
Sweepback, 50 percent chord line, degrees	0
Taper ratio	2.5:1
Mean aerodynamic chord -	
Length, inches	74.50
Location back of leading edge of root chord, inches	12.75
Root chord, inches	100
Tip chord, inches	40
Wing loading, W/S, pounds per square foot	25.7
Center of gravity:	
Back of leading edge of root chord, inches	30.80
Below reference line, inches	0.70
Percent of mean aerodynamic chord	24.2
Ratio of wing span to radius of gyration:	
b/k_X	7.43
b/k_Y	6.79
b/k_Z	5.13

TABLE I - (Continued)

DIMENSIONAL CHARACTERISTICS OF NACA SUBMERGED-ENGINE PUSHER AIRPLANE AS REPRESENTED BY 1/10-SCALE MODEL TESTED IN NACA FREE-FLIGHT TUNNEL

Flaps:	
Type -	
Zap extensible, partial span	
Span -	
Feet	16.77
Percent b	43.5
Percent chord	35.0
Aileron:	
Type -	
Plain	
Area	
Square feet	20
Percent S	8.8
Span	
Feet	15.6
Percent b	40
Tail:	
Horizontal -	
Area (includes fuselage) -	
Square feet	54
Percent S	24
Center of gravity to elevator hinge line, feet	13.5
Incidence, degrees	0
Span, feet	13
Elevator area, square feet	16.2
Above reference line, inches	13
Vertical (tails 1 and 2) -	
Total area (not including fuselage)	
Square feet	16.16
Percent S	7.2
Center of gravity to rudder hinge line, feet.	13.72
Span (each tail), feet	3.75
Rudder area (tail 1), square feet	7.37

TABLE II

AILERON EFFECTIVENESS OF NACA SUBMERGED-ENGINE PUSHER MODEL TESTED IN FREE-FLIGHT TUNNEL

Flap	pb/2V			
	25° total aileron deflection (a)		45° total aileron deflection (b)	
	Level flight (c)	Recovery (d)	Level flight (c)	Recovery (d)
Retracted (C_L = 0.5)	0.048	0.052	0.087	0.094
Extended (C_L = 0.8)	.067	.061	.121	.110

[a] Deflection used in abrupt aileron maneuvers. (Equal up-and-down deflection of ±12½°.) Rudder fixed.

[b] Assumed maximum aileron travel (±22½°). Values obtained by direct extrapolation from values for 25° deflection.

[c] Values obtained in abrupt aileron maneuvers starting from wing-level attitude.

[d] Values obtained during recoveries from abrupt aileron maneuvers.

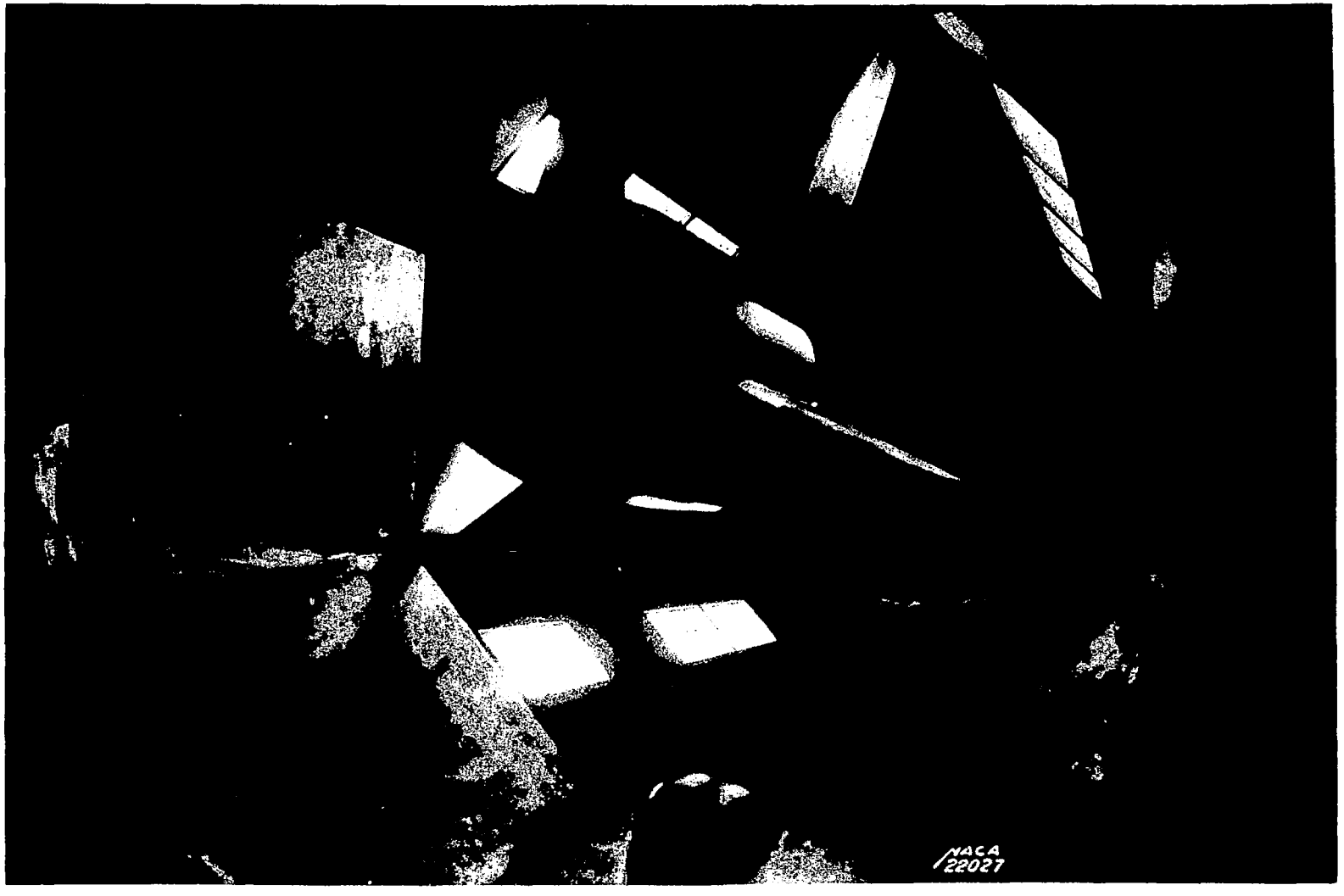

Figure 1.- Test section of the NACA free-flight tunnel showing a model being tested in flight.

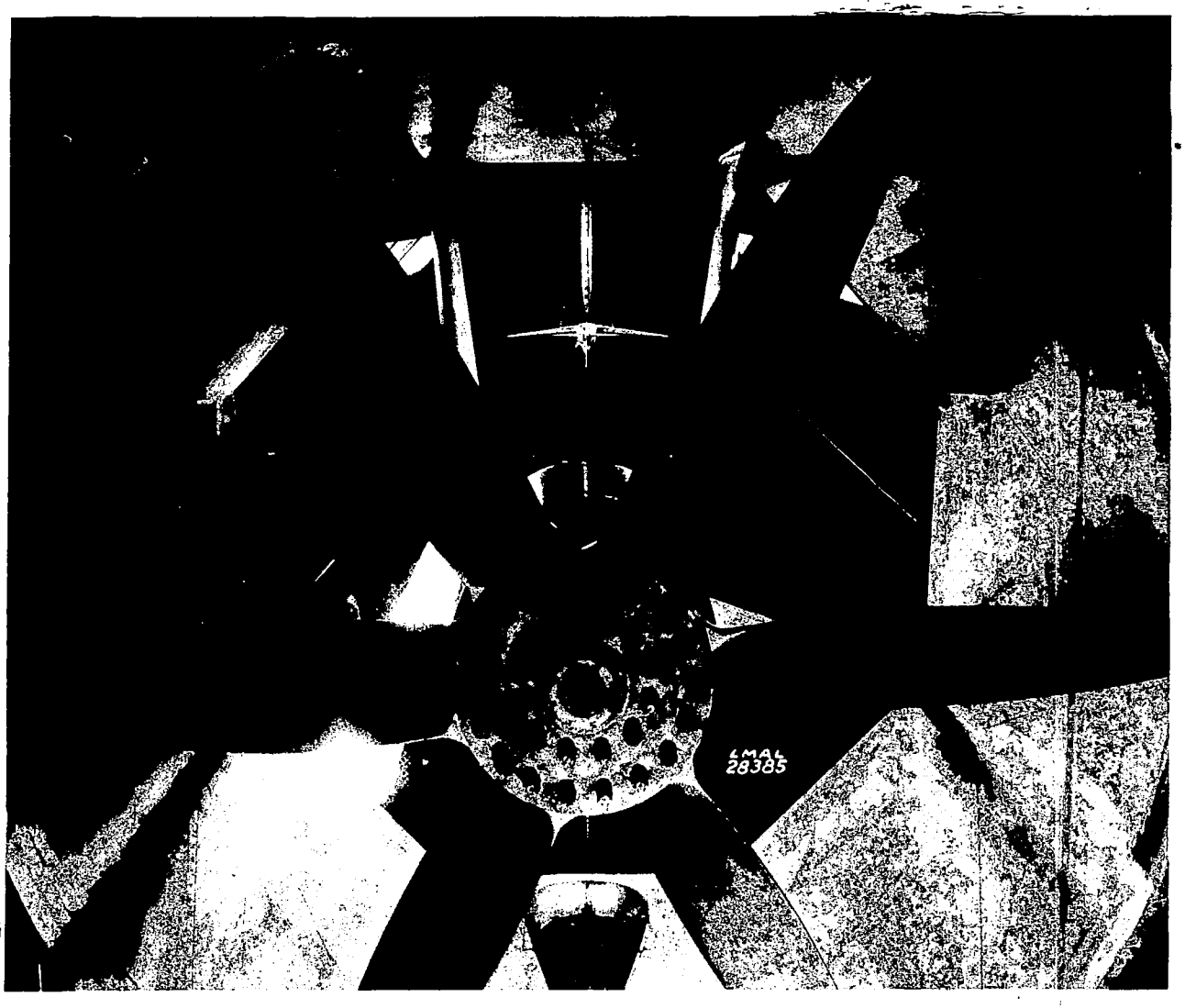

Figure 2.- Test section of NACA free-flight tunnel showing model mounted on a balance.

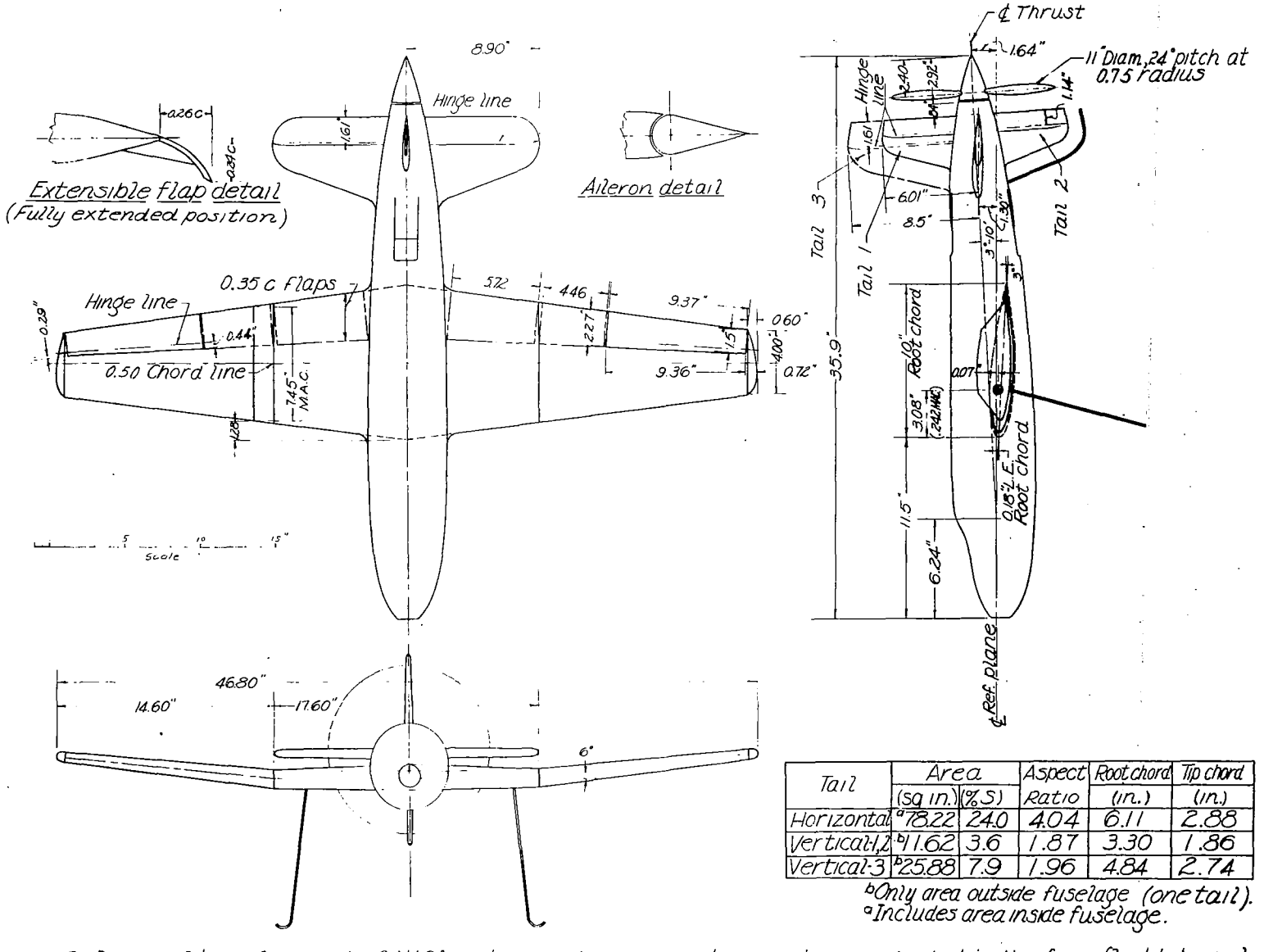

Tail	Area (sq in.)	Area (%S)	Aspect Ratio	Root chord (in.)	Tip chord (in.)
Horizontal	[a]78.22	24.0	4.04	6.11	2.88
Vertical-1,2	[b]11.62	3.6	1.87	3.30	1.86
Vertical-3	[b]25.88	7.9	1.96	4.84	2.74

[b]Only area outside fuselage (one tail).
[a]Includes area inside fuselage.

FIGURE 3.—Drawing of 1/10-scale model of NACA submerged-engine pusher airplane as tested in the free-flight tunnel.

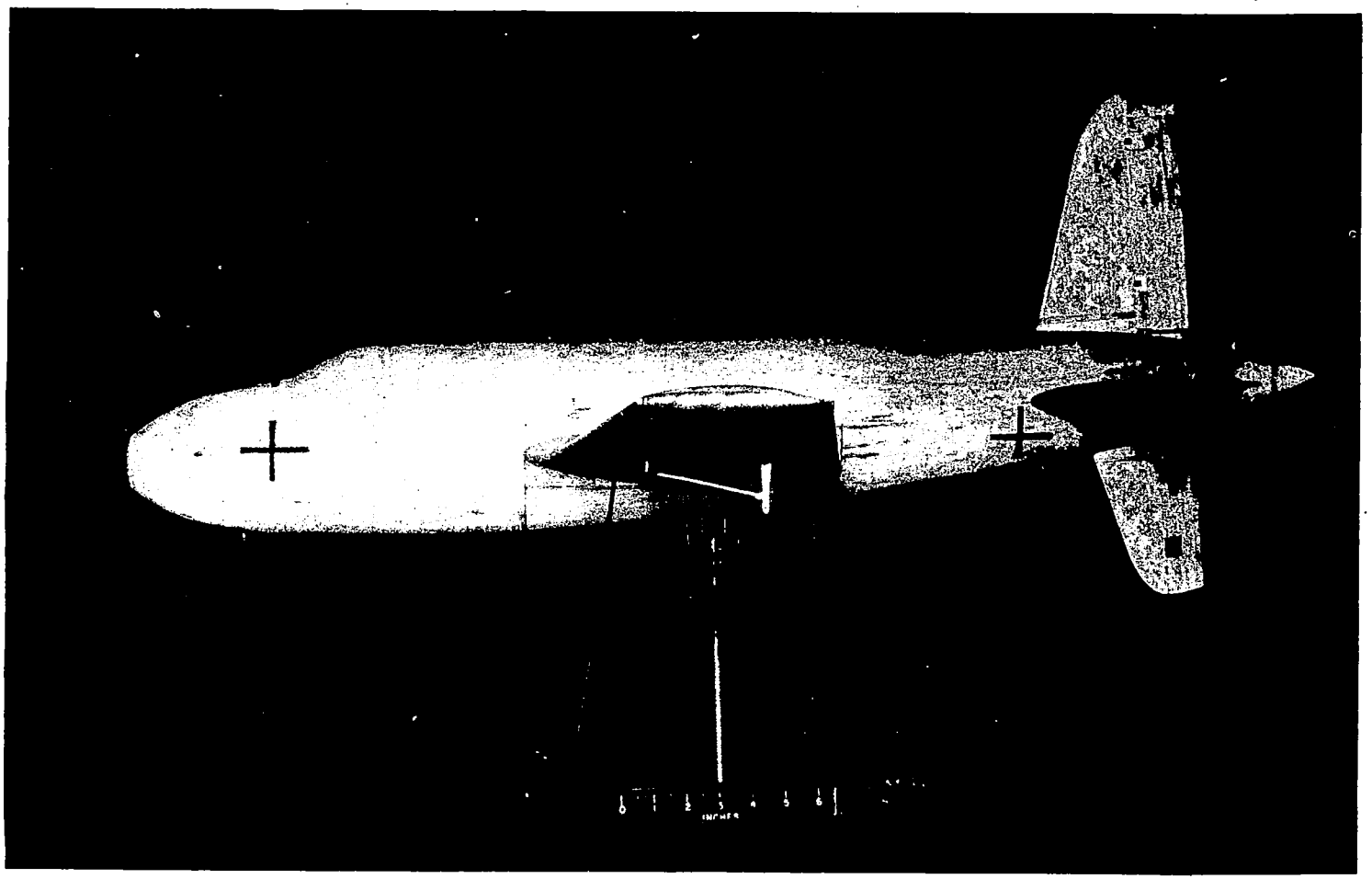

Figure 4.- Side elevation of 1/10-scale model of NACA submerged-engine pusher airplane as originally tested in free-flight tunnel with small lower vertical tail (tail 2) and large upper vertical tail (tail 3).

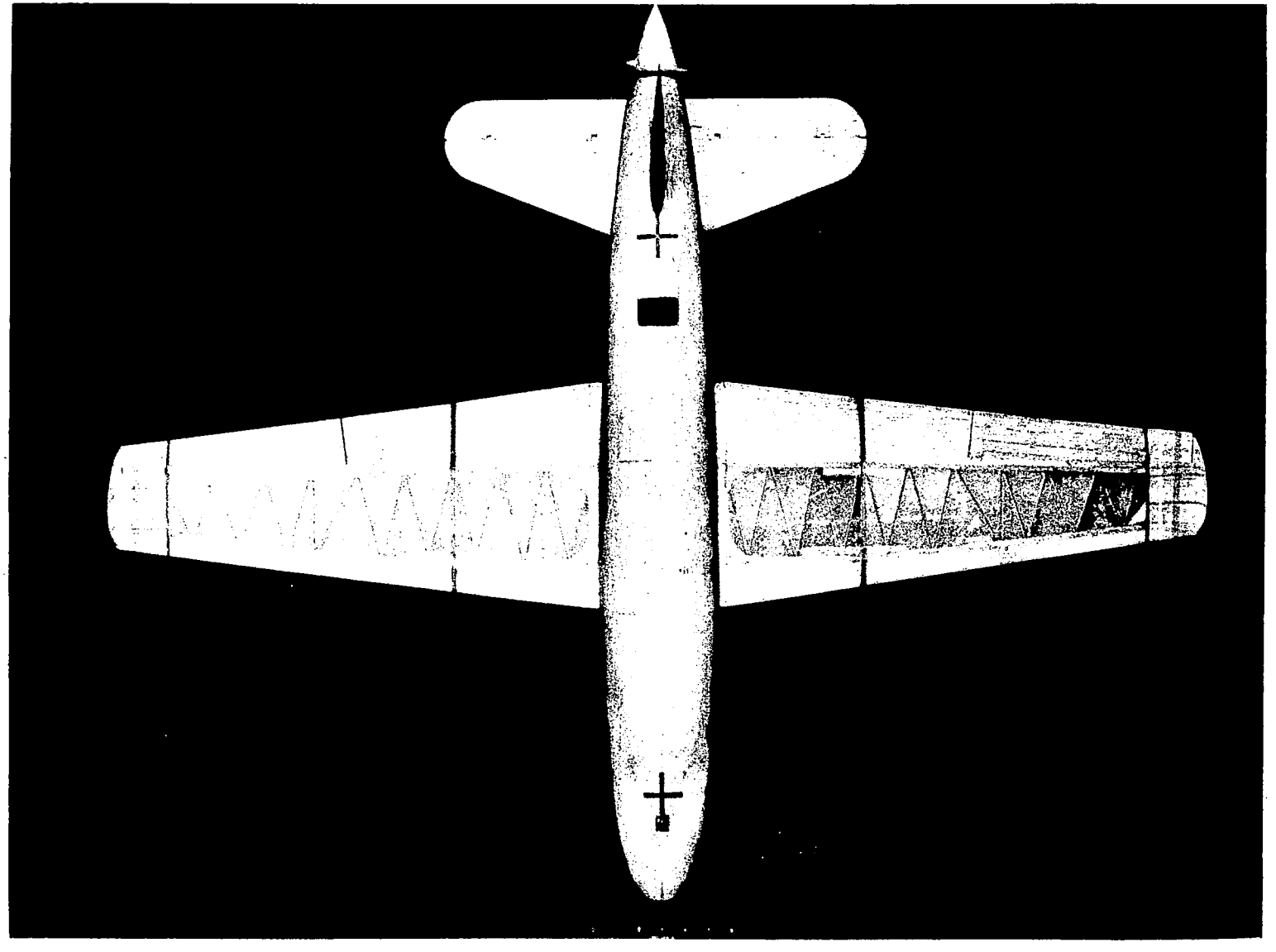

Figure 5.- Plan view of 1/10-scale model of NACA submerged-engine pusher airplane as originally tested in the free-flight tunnel.

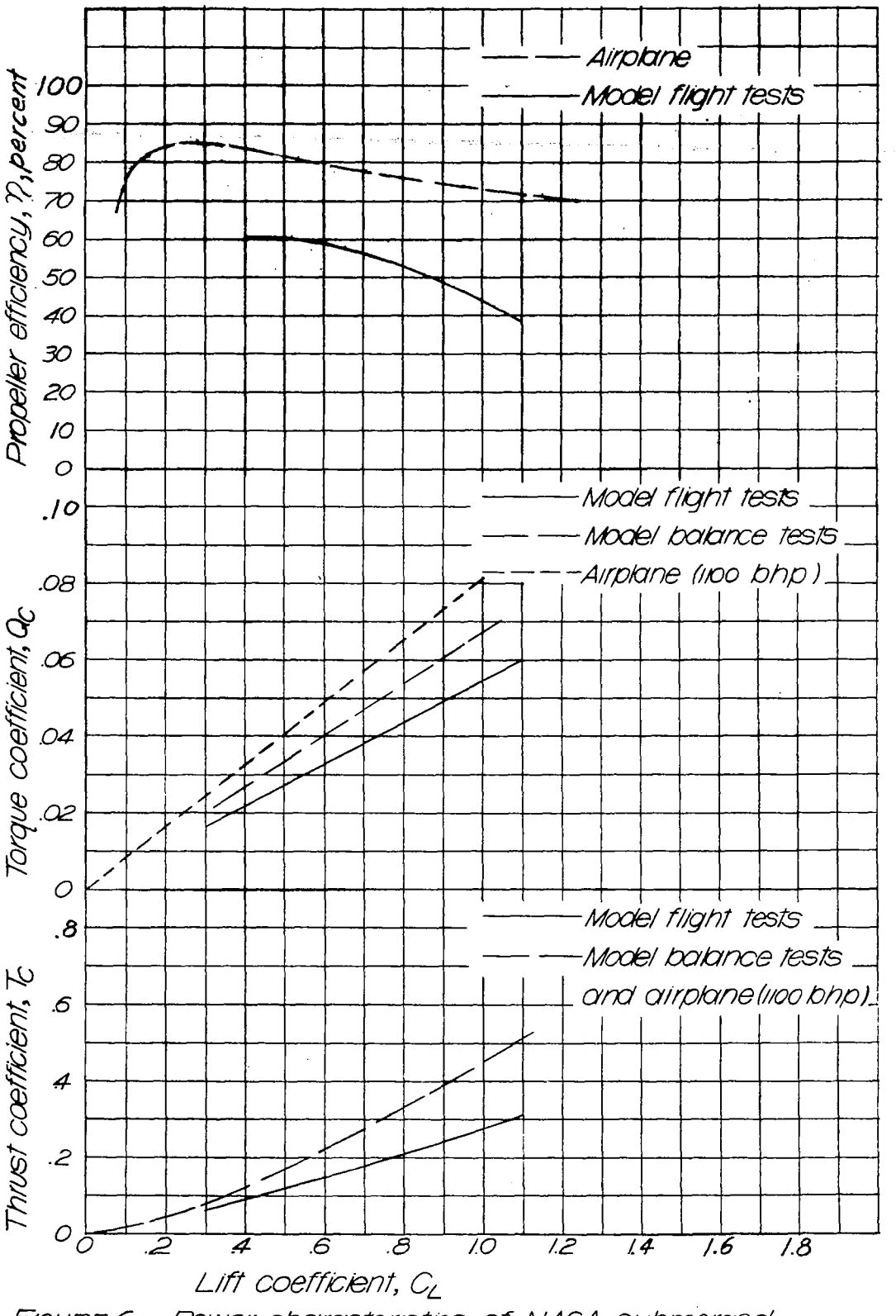

FIGURE 6.–Power characteristics of NACA submerged-engine pusher model tested in NACA free-flight tunnel.

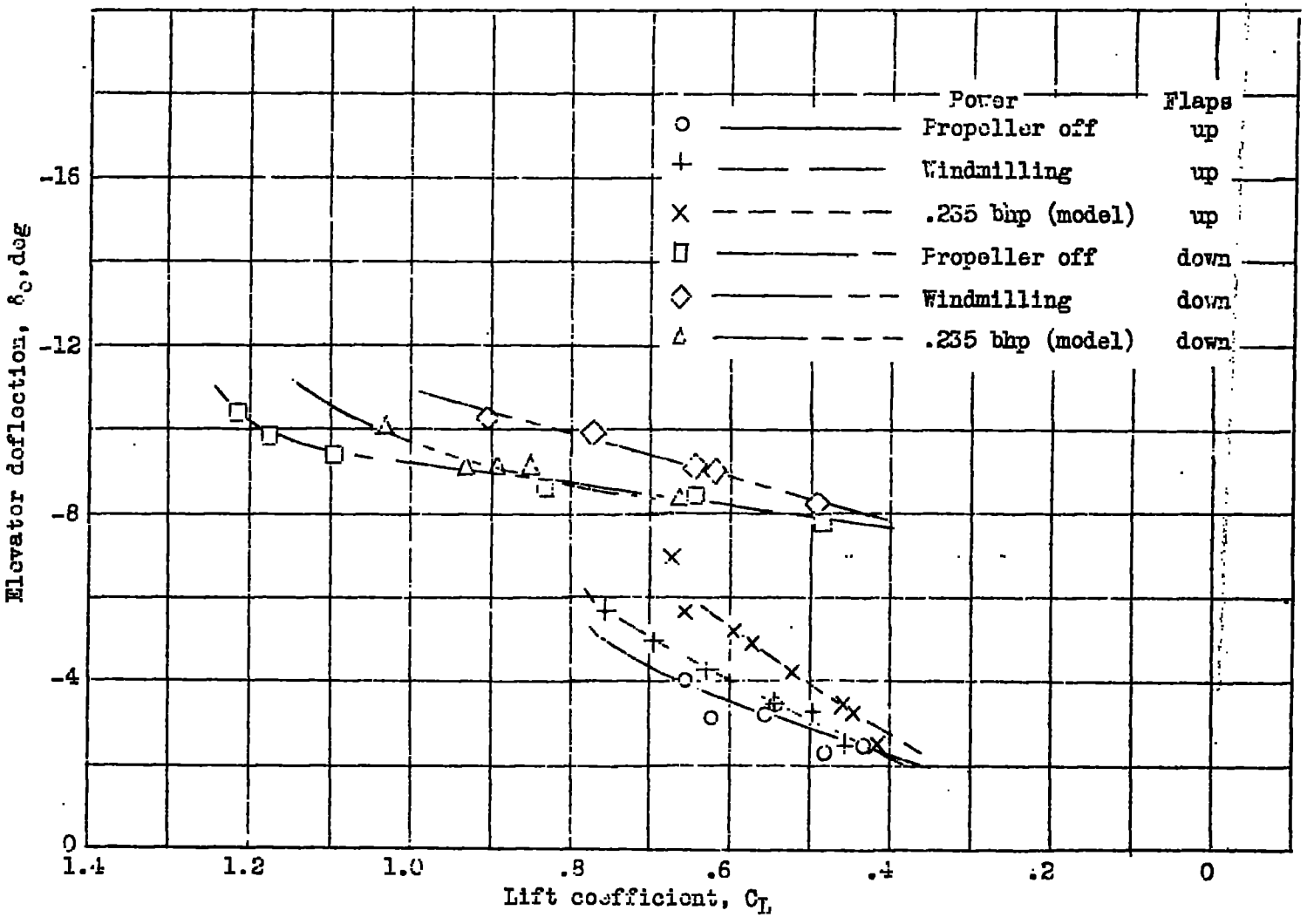

Figure 7.- Effect of power and flaps on longitudinal stability and trim characteristics of NACA submerged-engine pusher model as determined by flight tests in the NACA free-flight tunnel. $i_t = 0°$.

NACA

Fig. 8

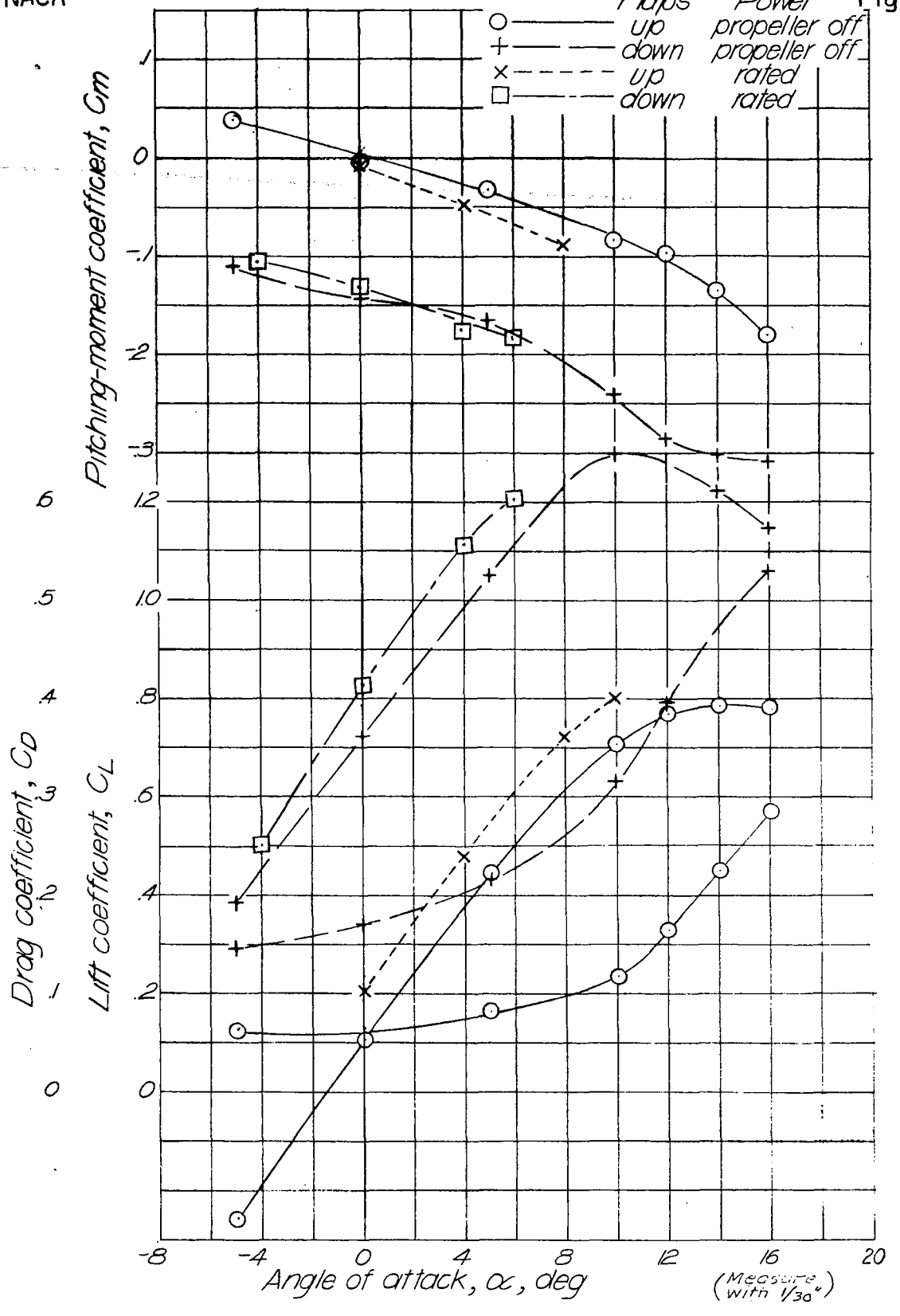

FIGURE 8.- Effect of power and flaps on aerodynamic characteristics of NACA submerged-engine pusher model as determined by balance tests in the NACA free-flight tunnel. $i_t = 0°$; $\delta_e = 0°$.

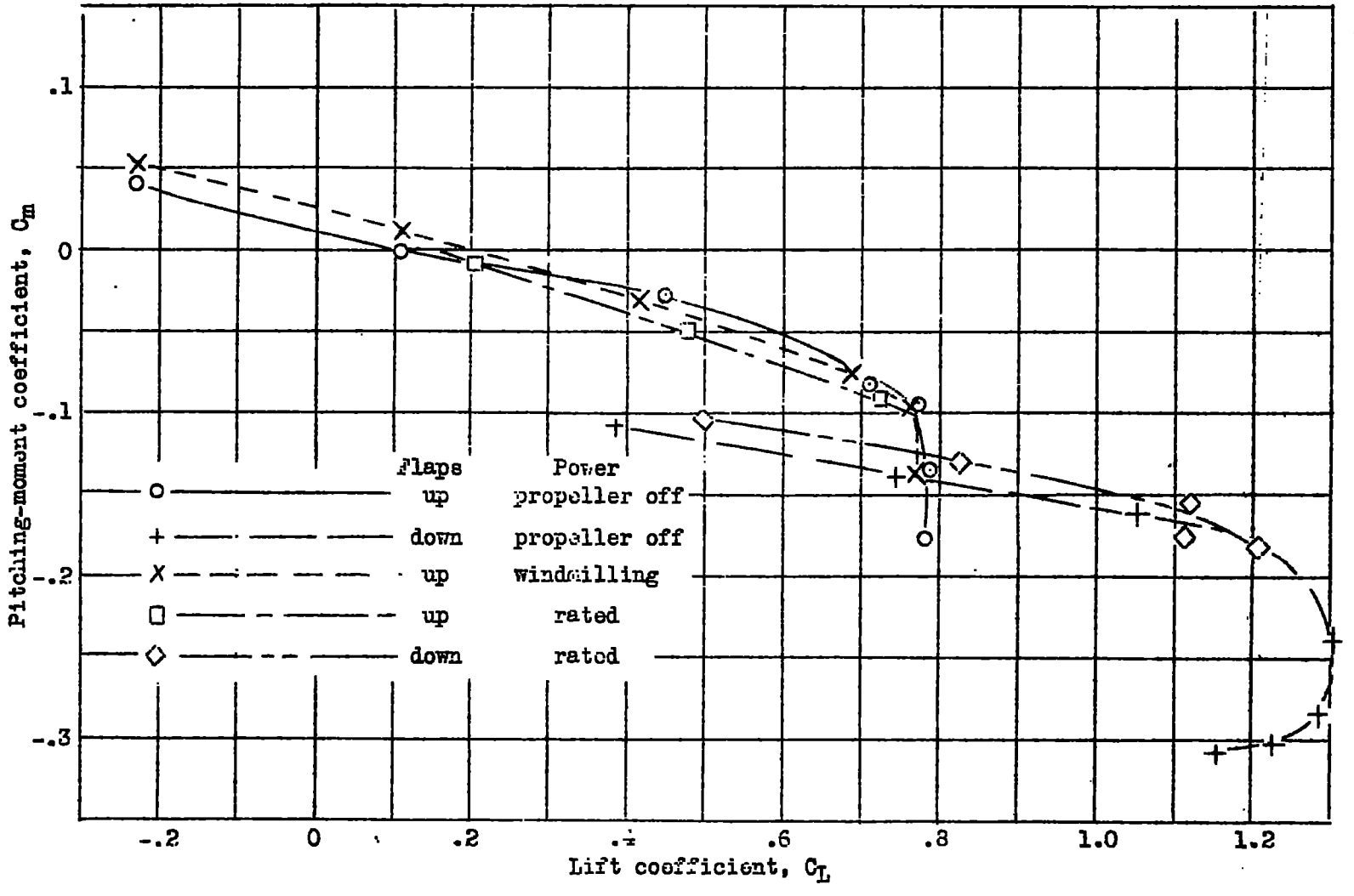

Figure 9.- Effect of power and flaps on longitudinal stability and trim characteristics of NACA submerged-engine pusher model as determined by balance tests in the NACA free-flight tunnel. $i_t = 0^\circ$; $\delta_e = 0^\circ$.

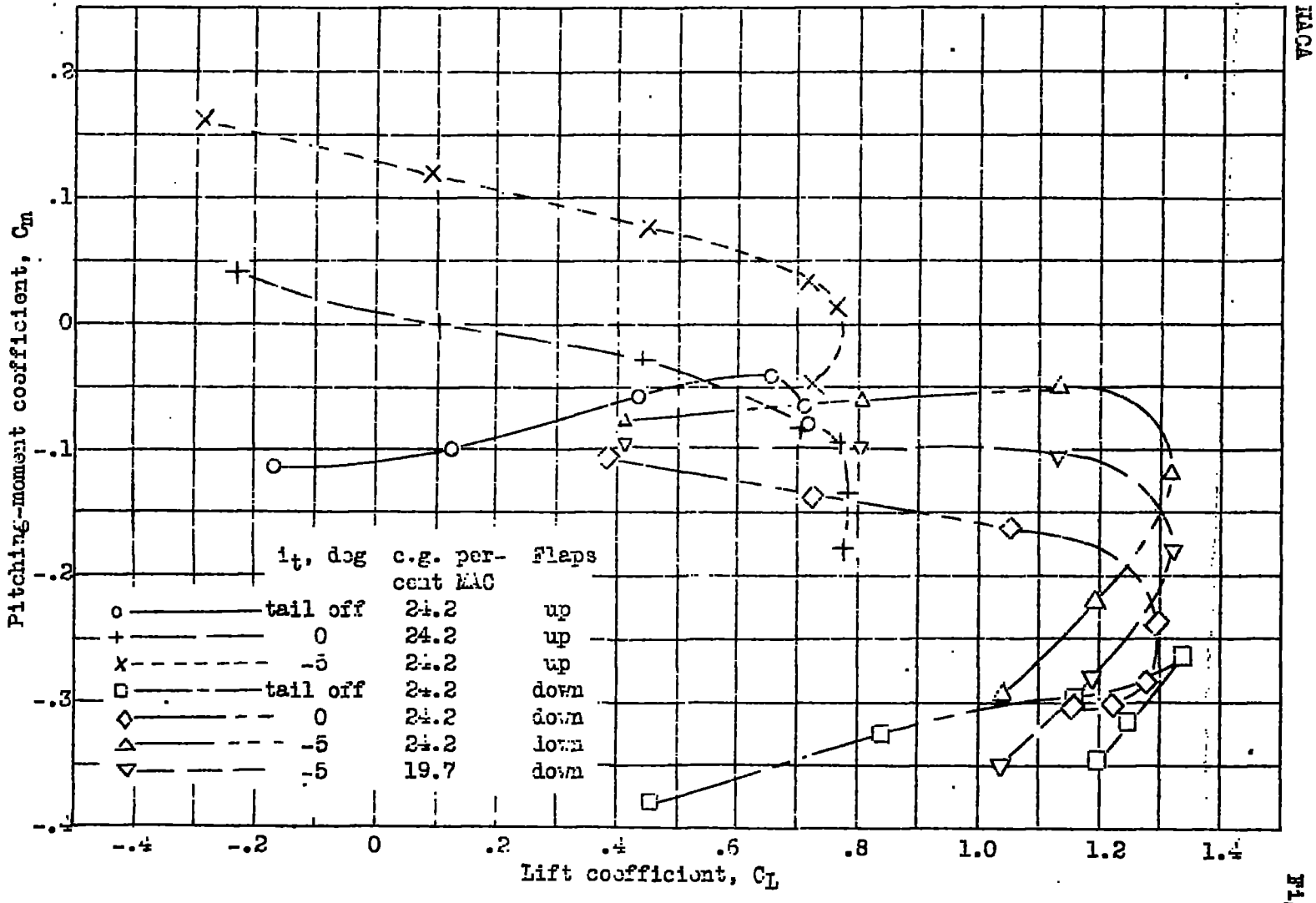

Fig. 10

Figure 10.- Effect of horizontal-tail incidence and center-of-gravity location on longitudinal stability characteristics of NACA submerged-engine pusher model tested in NACA free-flight tunnel. Propeller off.

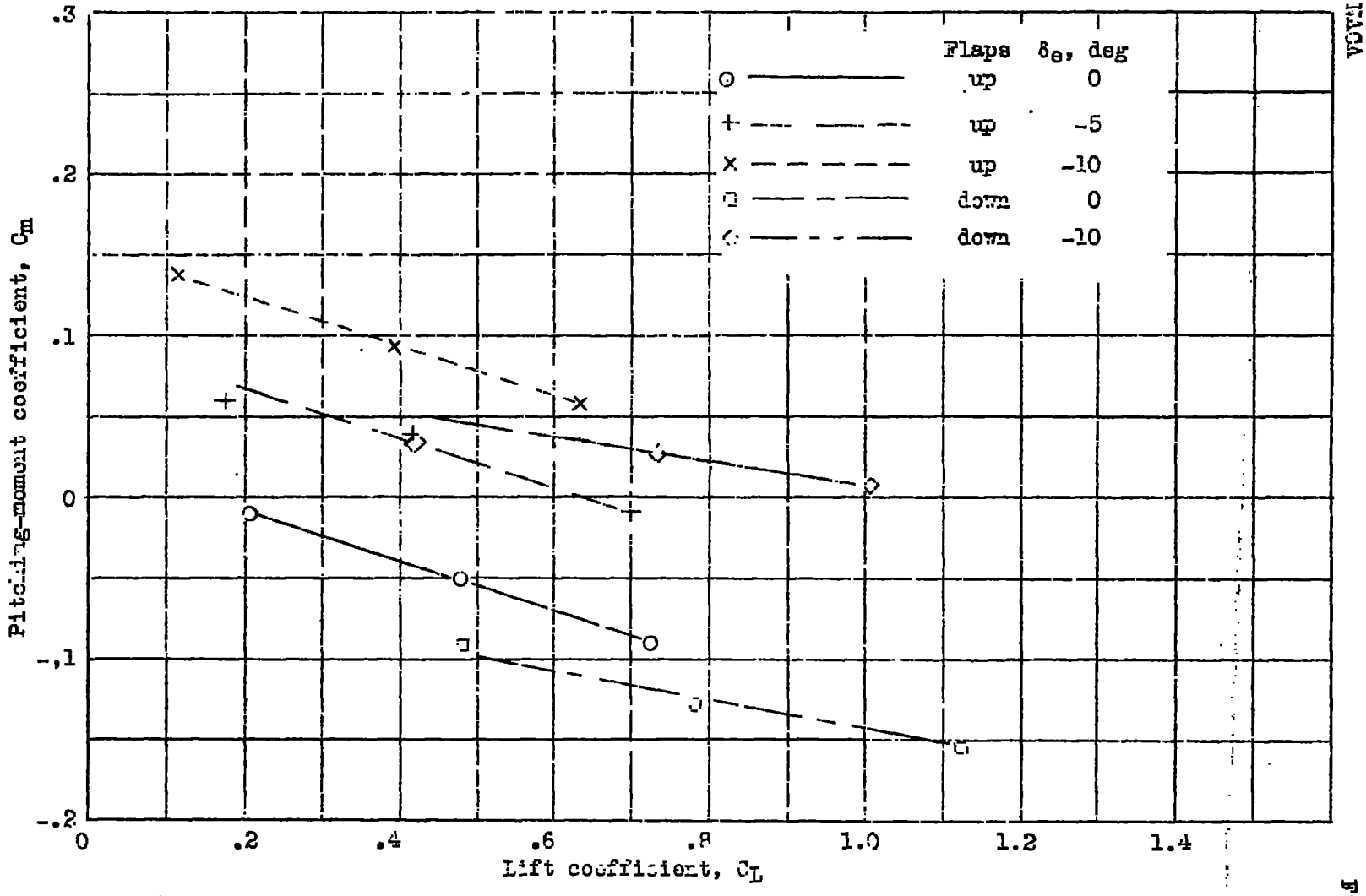

Figure 11.- Elevator effectiveness of NACA submerged-engine pusher model as determined by balance tests in NACA free-flight tunnel. Rated power, $i_t = 0^\circ$.

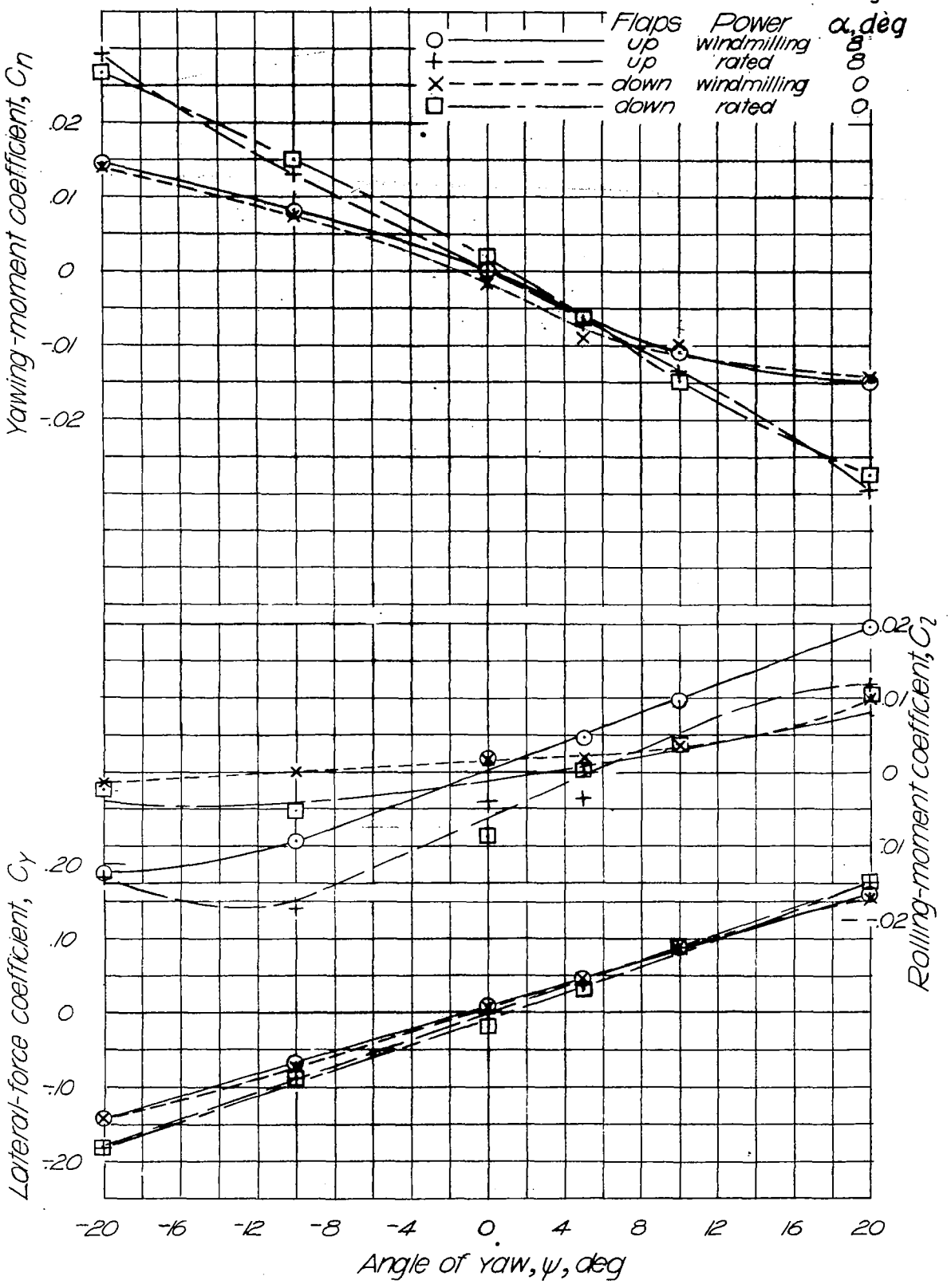

FIGURE 12.- Effect of flaps and power on lateral-stability characteristics of NACA submerged-engine pusher model tested in the NACA free-flight tunnel. Vertical tails 1 and 2 on. (Balance data)

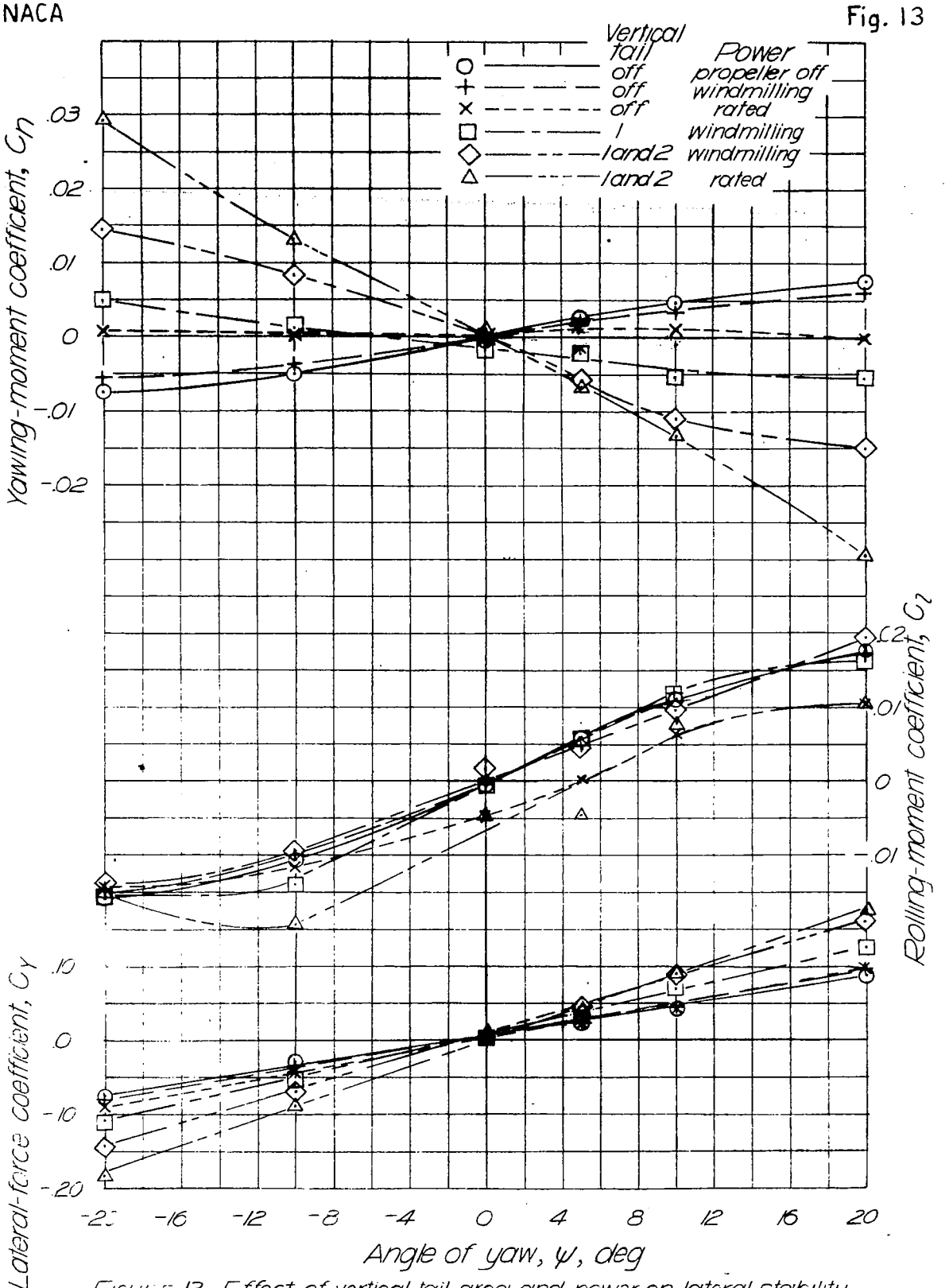

FIGURE 13–Effect of vertical-tail area and power on lateral-stability characteristics of NACA submerged-engine pusher model as determined by balance tests in the NACA free-flight tunnel. Flaps retracted; $\alpha = 8°$.

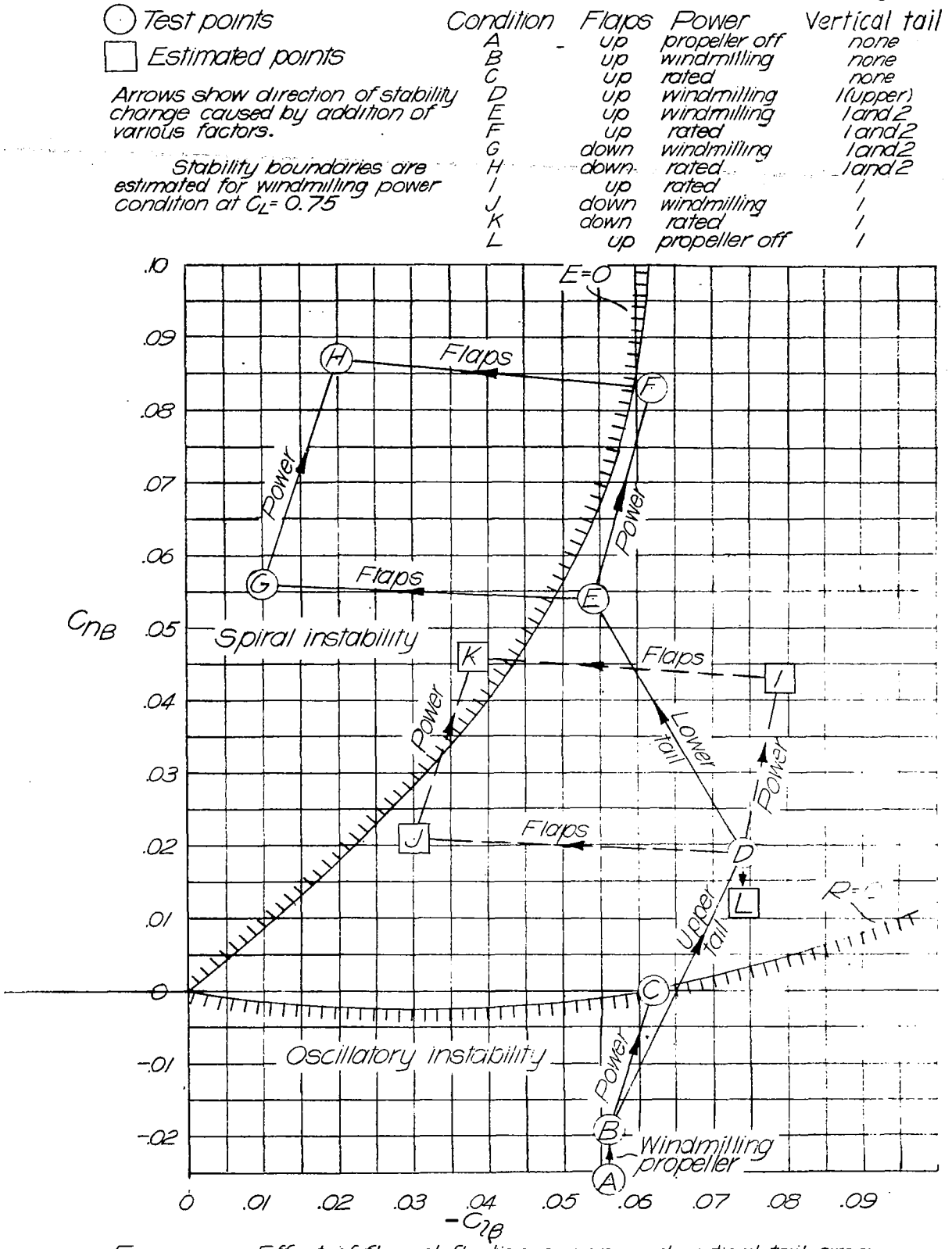

FIGURE 14.- Effect of flap deflection, power, and vertical-tail area on the lateral stability of the NACA submerged-engine pusher model tested in the free-flight tunnel. $C_L = 0.75$.

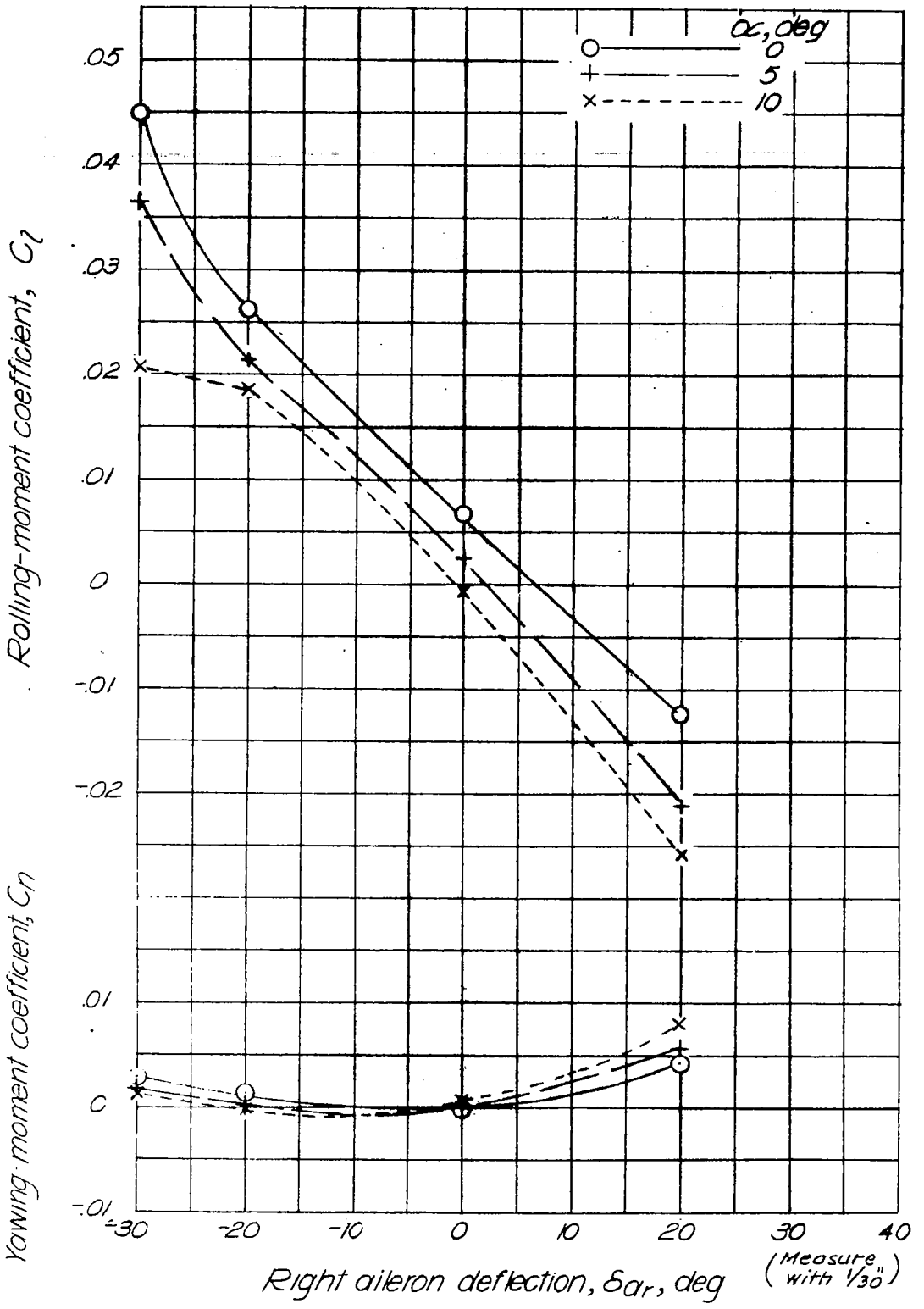

FIGURE 15.– Aileron effectiveness of NACA submerged-engine pusher model as determined by balance tests in the free-flight tunnel. Propeller windmilling; flaps retracted.

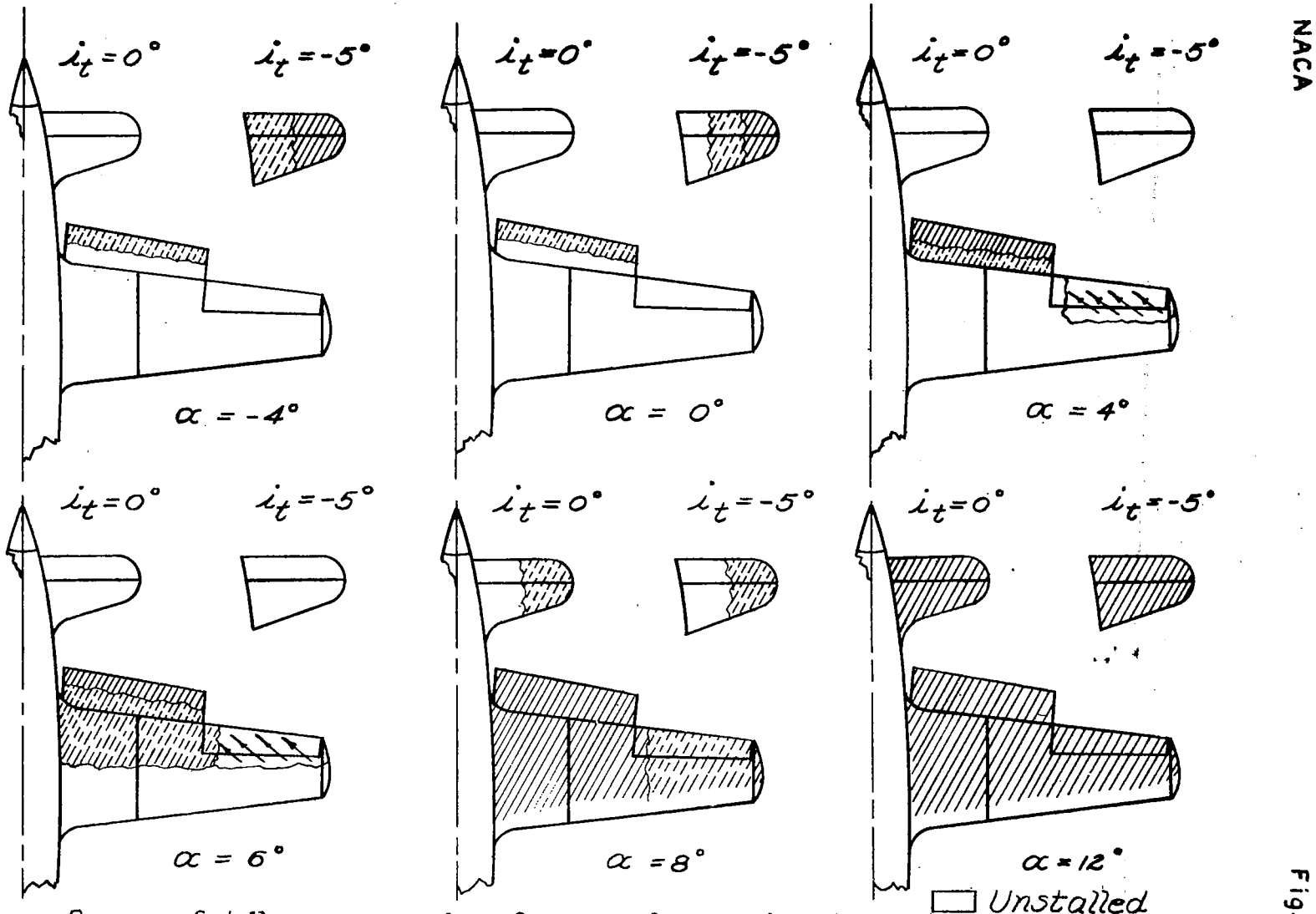

FIGURE 16.—Progress of stall on upper surface of wing and lower surface of horizontal tail of free-flight-tunnel model of NACA submerged-engine pusher airplane. Flaps down; propeller windmilling.